

Article

# Structures of Reaction Products and Degradation Pathways of Aflatoxin B<sub>1</sub> by Ultrasound Treatment

Yuanfang Liu <sup>1,2</sup>, Mengmeng Li <sup>1</sup>, Yuanxiao Liu <sup>1</sup> and Ke Bian <sup>1,\*</sup><sup>1</sup> College of Food Science and Technology, Henan University of Technology, Zhengzhou 450001, China<sup>2</sup> School of Chemistry and Chemical Engineering, Zhengzhou Normal University, Zhengzhou 450044, China

\* Correspondence: kebian@haut.edu.cn; Tel.: +86-371-6775-6889

Received: 16 August 2019; Accepted: 10 September 2019; Published: 12 September 2019



**Abstract:** Ultrasound is an emerging decontamination technology with potential use in the global food processing industry. In the present study, we explored power ultrasound for processing aqueous aflatoxin B<sub>1</sub> (AFB<sub>1</sub>). AFB<sub>1</sub> was degraded by 85.1% after 80 min of ultrasound exposure. The reaction products of AFB<sub>1</sub> were identified and their molecular formulae elucidated by ultra-high-performance liquid chromatography Q-Orbitrap mass spectrometry. Eight main reaction products were found, and their structures were clarified by parental ion fragmentation. Two degradation pathways were proposed according to the degradation product structures: One involved the addition of H• and OH• radicals, whereas the other involved H<sub>2</sub>O<sub>2</sub> epoxidation and H•, OH•, and H<sub>2</sub>O<sub>2</sub> oxidation of AFB<sub>1</sub>. Ultrasound treatment significantly reduced AFB<sub>1</sub> bioactivity and toxicity by disrupting the C8=C9 double bond in the furan ring and modifying the lactone ring and methoxy group.

**Keywords:** reaction products; aflatoxin B<sub>1</sub>; UHPLC-Orbitrap-MS; ultrasound treatment

**Key Contribution:** Ultrasound treatment reduced aflatoxin B<sub>1</sub> toxicity in aqueous solutions by disrupting the C8=C9 double bond in the furan ring; and modifying the lactone ring and methoxy group. This study establishes a foundation to use pulsed ultrasound as a novel; economic; and environment-friendly technique for efficiently removing mycotoxins from food and feed.

## 1. Introduction

Aflatoxins are the most common mycotoxins. They are secondary metabolites of *Aspergillus flavus* that can reduce food quality [1] and have adverse health effects [2,3]. Aflatoxin B<sub>1</sub> (AFB<sub>1</sub>) is the strongest teratogen, mutagen, and hepatocarcinogen known. The International Agency for Research on Cancer (IARC) has rated AFB<sub>1</sub> as a class 1 carcinogen [4]. AFB<sub>1</sub> is distributed mainly in maize, peanut, rice, wheat, and other crops, as well as in their oil-based by-products. Small quantities of AFB<sub>1</sub> are also found in dairy products and condiments [5].

Prevention of mycotoxin contamination is the most economically effective way of reducing the risks posed by aflatoxin exposure. However, additional processing is often insufficient for the decontamination and detoxification of food and feed products. Detoxification is important in making aflatoxin-contaminated grains usable, and thus, safeguarding the food industry. Over the last several decades, physical, biological, and chemical strategies for aflatoxin degradation and their effects on aflatoxin content have been extensively investigated [6–8]. Detoxification treatments include electron beam irradiation [9], citric and lactic acids [10], ozone gas [11], cold plasma [12], and neutral electrolytic water [13]. However, most methods have disadvantages, such as nutrient loss, inconvenience of operation, reduction of sensory attributes, and high costs. Consequently, these techniques are of little practical use. Thus, there is a high demand for effective, specific, and environment-friendly technologies in this regard.

Ultrasound is emerging as an environment protection method, as it produces no secondary pollutants [14]. Cavitation bubbles in liquid media are generated by ultrasound when acoustic wave occurs during the rarefaction cycle. The bubbles continue to expand until they collapse after reaching a critical radius [15]. When cavitation bubbles collapse, they raise the temperature to  $>5000\text{ }^{\circ}\text{C}$  and the pressure to  $>1000\text{ atm}$  [16]. Under these extreme conditions, contaminant compounds in the vicinity are degraded. The covalent bonds in water are broken, and  $\text{OH}\bullet$  radicals are formed. These radicals oxidize aqueous contaminants [15]. Ultrasound treatment has received increasing attention as a means of degrading various micropollutants, such as parathion [17], 5-methylbenzotriazole [18], ibuprofen [19], and ethyl paraben [20]. To the best of our knowledge, however, there has been no extensive study on the reaction products of  $\text{AFB}_1$  treated with ultrasound or their potential toxicity. Thus, little is known about the reaction mechanisms involved in the degradation of  $\text{AFB}_1$  by ultrasound treatment, and elucidation of the ultrasound process is the basis for the development of its future applications. This study is a continuation of a previous investigation of the treatment of mycotoxins ( $\text{AFB}_1$ , deoxynivalenol, zearalenone, and ochratoxin A) with ultrasound [21]. The goals of this study were to identify the molecular structures of the reaction products of  $\text{AFB}_1$ , elucidate the decomposition mechanisms and reaction pathways of  $\text{AFB}_1$ , and determine the particular factors that lead to  $\text{AFB}_1$  degradation. Toxicity of the reaction products was also correlated with their structures.

## 2. Results and Discussion

### 2.1. Formation of $\text{AFB}_1$ Reaction Products as A Function of Ultrasound Treatment Time

Chromatography/mass spectrometry data for  $\text{AFB}_1$  before and after ultrasound treatment were collected by UHPLC-Q-Orbitrap high-resolution mass spectrometry (Orbitrap MS-MS). MS/MS fragment ion data were collected simultaneously. The original data were imported into SIEVE v. 2.0 (Thermo Fisher Scientific, Bremen, Germany) for differential expression analysis. The software identified eight new products generated after 40 min of US treatment of  $\text{AFB}_1$ , which was mainly degraded; these were labeled P1–P8 (Figure 1). Their signal-to-noise ratios were below the detection threshold in the blank experiment. Figure 1C,D shows that the retention times and peak shapes of the eight reaction products were satisfactorily separated. Their response values were sufficiently high for detection. The compounds were found in the samples after 30, 40, 60, and 80 min of ultrasound treatment.

Figure 2 shows the changes in the responses of  $\text{AFB}_1$  and its reaction products (P1–P8) in water with increasing US treatment time.  $\text{AFB}_1$  gradually decomposed with increasing treatment time. The levels of all reaction products except P2 and P7 gradually increased within the first 40 min of US treatment and decreased thereafter. The observed decreases in the levels of certain degradation product suggest that these substances may have been reaction intermediates subsequently converted to other reaction products. There was a tremendous decay trend after the observed decrease in  $\text{AFB}_1$  level during the 40-min ultrasound treatment. This finding is in line with our previous findings for aflatoxin B<sub>1</sub> subjected to ultrasound treatment [21]. The areas of the peaks indicated that ~85.1% of the  $\text{AFB}_1$  was degraded after 80 min of ultrasound treatment.

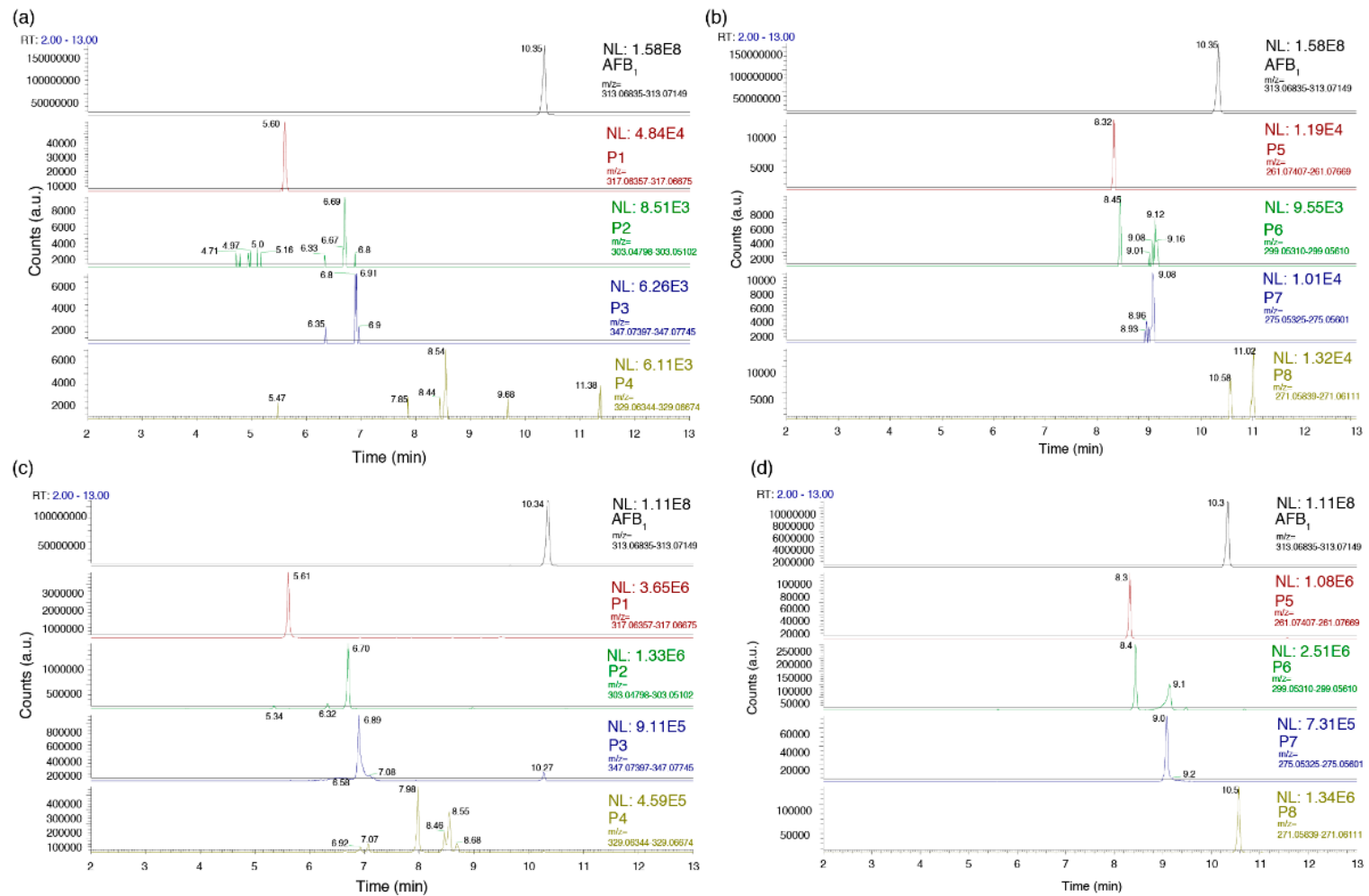


**Figure 1.** Total-ion chromatograms of untreated Aflatoxin B<sub>1</sub> (AFB<sub>1</sub>) (10 µg·mL<sup>-1</sup>) in ultrapure water (a,b) and AFB<sub>1</sub> in ultrapure water exposed to ultrasound for 40 min (c,d).

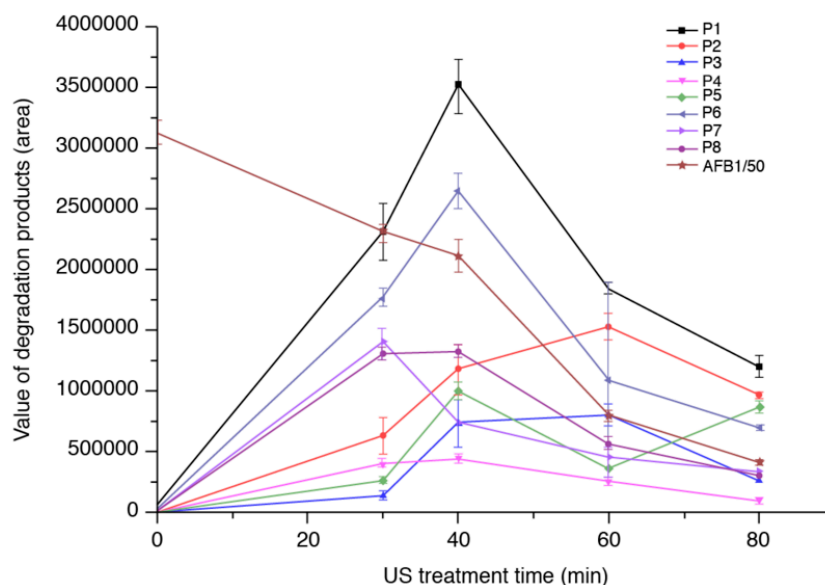


**Figure 2.** Relative change in the responses of AFB<sub>1</sub> and its reaction products (P1–P8) in water with increasing ultrasound (US) treatment time. (Note: The AFB<sub>1</sub> values were normalized so they could be displayed in the same scale.)

## 2.2. Molecular Formulae of the AFB<sub>1</sub> Reaction Products

To help identify the molecular formulae of the reaction products of AFB<sub>1</sub>, their retention times, proposed formulae, experimental masses, mass errors, index of hydrogen deficiency (IHD), and score data, as well as those for AFB<sub>1</sub>, are summarized in Table 1. The overall score ranged from 0–100%. Scores closer to 100% were preferable. Relative to the ideal mass gained from the hypothetical molecular formula, the mass measured by the Q-Orbitrap-MS experiments had an error <0.5 mmu.

**Table 1.** Hypothetical formulae for the AFB<sub>1</sub> reaction products.

Proposed Product	Retention Time (min)	Hypothetical Formula	Determined Mass ( <i>m/z</i> ) <sup>1</sup>	Error (mmu)	IHD <sup>2</sup>	Score (%)
1	5.69	C <sub>16</sub> H <sub>13</sub> O <sub>7</sub>	317.06516	−0.419	10.5	89.1
2	6.82	C <sub>15</sub> H <sub>11</sub> O <sub>7</sub>	303.04950	−0.429	10.5	87.6
3	6.99	C <sub>17</sub> H <sub>15</sub> O <sub>8</sub>	347.07571	−0.434	10.5	88.9
4	7.17	C <sub>17</sub> H <sub>13</sub> O <sub>7</sub>	329.06509	−0.487	11.5	92.5
5	8.42	C <sub>14</sub> H <sub>13</sub> O <sub>5</sub>	261.07538	−0.370	8.5	88.3
6	8.54	C <sub>16</sub> H <sub>11</sub> O <sub>6</sub>	299.05460	−0.415	11.5	90.9
7	9.21	C <sub>14</sub> H <sub>11</sub> O <sub>6</sub>	275.05463	−0.385	9.5	82.5
8	10.68	C <sub>15</sub> H <sub>11</sub> O <sub>5</sub>	271.05975	−0.350	10.5	85.2
AFB <sub>1</sub>	10.45	C <sub>17</sub> H <sub>12</sub> O <sub>7</sub>	313.07025	−0.415	11.5	99.2

<sup>1</sup> *m/z* of [M + H]<sup>+</sup>. <sup>2</sup> IHD: Index of hydrogen deficiency.

As accurate masses of these eight reaction products were generated by SIEVE v. 2.0 (Thermo Fisher Scientific, Waltham, MA, USA), their elemental compositions could be speculated by considering all possible permutations. AFB<sub>1</sub> was processed by ultrasound treatment in pure water. Thus, the reaction products of AFB<sub>1</sub> should only be formed of hydrogen, carbon, and oxygen. The molecular formulae were predicted by Xcalibur v. 3.0 (Thermo Fisher Scientific) and according to exact masses of the compounds. For example, some possible molecular compositions of P-1 were C<sub>16</sub>H<sub>13</sub>O<sub>7</sub>, C<sub>12</sub>H<sub>13</sub>O<sub>10</sub>, and C<sub>17</sub>H<sub>17</sub>O<sub>6</sub> with scores of 89.1, 85.1, and 80.4%, respectively. As C<sub>16</sub>H<sub>13</sub>O<sub>7</sub> showed a higher score than the others, it is most possibly the correct molecular formula for P-1. The IHD of the reaction products of AFB<sub>1</sub> should be closer to that of AFB<sub>1</sub>. The IHD of AFB<sub>1</sub> is 11.5, and there are 17 carbon atoms and 12 hydrogen atoms in one AFB<sub>1</sub> molecule. The IHDs of the molecular formulae C<sub>16</sub>H<sub>13</sub>O<sub>7</sub>,

$C_{12}H_{13}O_{10}$ , and  $C_{17}H_{17}O_6$  are 10.5, 6.5, and 9.5, respectively. As the IHD of  $C_{16}H_{13}O_7$  most nearly approaches that of AFB<sub>1</sub>, it is the most likely molecular formula for P-1.

### 2.3. Proposed Structures of the AFB<sub>1</sub> Reaction Products

To elucidate the structures of the eight reaction products of AFB<sub>1</sub>, the exact masses of their fragmentation ions were evaluated by Orbitrap MS–MS. In this way, the most probable structures of the reaction products of AFB<sub>1</sub> and their parent compounds could be determined. Based on the parent ions' masses and fragments gained from MS–MS, the structures of the eight reaction products are displayed in Figure 3. The structures of the AFB<sub>1</sub> reaction products, generated by US treatment, are shown in Figure 4. The structures of the eight reaction products (P1–P8) resemble that of AFB<sub>1</sub>. US treatment modified the AFB<sub>1</sub> furofuran ring (P-1–P-5 and P-7), lactone ring (P-2, P-3, and P-8), and methoxy group (P-1, P-2, P-6, and P-8).

### 2.4. Degradation Mechanism and Reaction Pathway of AFB<sub>1</sub> upon US Treatment

High-power ultrasound treatment modifies the physicochemical properties of food-borne pathogens during processing [22]. The ultrasound treatment causes cavitation in which the covalent bonds of water molecules are broken, and numerous free radicals are generated that oxidize contaminants in water [15]. The temperature of the sample treated with ultrasound is ~60 °C, which is below the temperature required for thermal degradation of AFB<sub>1</sub> in water (120 °C) [23]. The heat generated during ultrasound treatment has a negligible effect on AFB<sub>1</sub> degradation. We believe that the free radicals, generated during ultrasound treatment, lead to the degradation of AFB<sub>1</sub>. Furthermore, it should be noted that the temperature rises by cavitation, as discussed previously, occurs solely in the mini bubbles generated; however, the temperature change, in this case, is stable, continuous, and uniform.



Ultrasound treatment generates numerous hydroxyl radicals (Reaction 1). At low mycotoxin concentrations, the hydroxyl radicals combine to form hydrogen peroxide (Reaction 2). At suitably high AFB<sub>1</sub> concentrations, the hydroxyl radicals degrade the mycotoxin molecules (Reaction 3). Sonolysis of water yields free radicals, such as hydrogen atoms and hydroxyl, as well as hydrogen peroxide [24,25]. Under ultrasound treatment with cavitation, the water molecules are broken into free radicals, which degrade various micropollutants, such as parathion [17], 5-methylbenzotriazole [18], ibuprofen [19], and ethyl paraben [20]. Sonolysis generates highly reactive hydroxyl radicals, which recombine outside of the bubbles even at very low scavenger concentrations to form hydrogen peroxide that is released into the medium [25]. The hydroxyl radicals may also attack AFB<sub>1</sub> and initiate its degradation. Aflatoxins are also effectively degraded by aqueous ozone because it too generates hydroxyl radicals [26,27]. The AFB<sub>1</sub> reaction products P-1 ( $C_{16}H_{13}O_7$ ) and P-3 ( $C_{17}H_{15}O_8$ ) are the major by-products of AFB<sub>1</sub> treatment with aqueous ozone [26,28]. The AFB<sub>1</sub> reaction products P-4 ( $C_{17}H_{13}O_7$ ), P-5 ( $C_{14}H_{13}O_5$ ), and P-7 ( $C_{14}H_{11}O_6$ ) are the reaction products of AFB<sub>1</sub> treated with high-voltage atmospheric cold plasma [29]. In this study, we identified additional major reaction products of AFB<sub>1</sub>. Thus, degradation of AFB<sub>1</sub> by ultrasound treatment sheds light on new pathways.

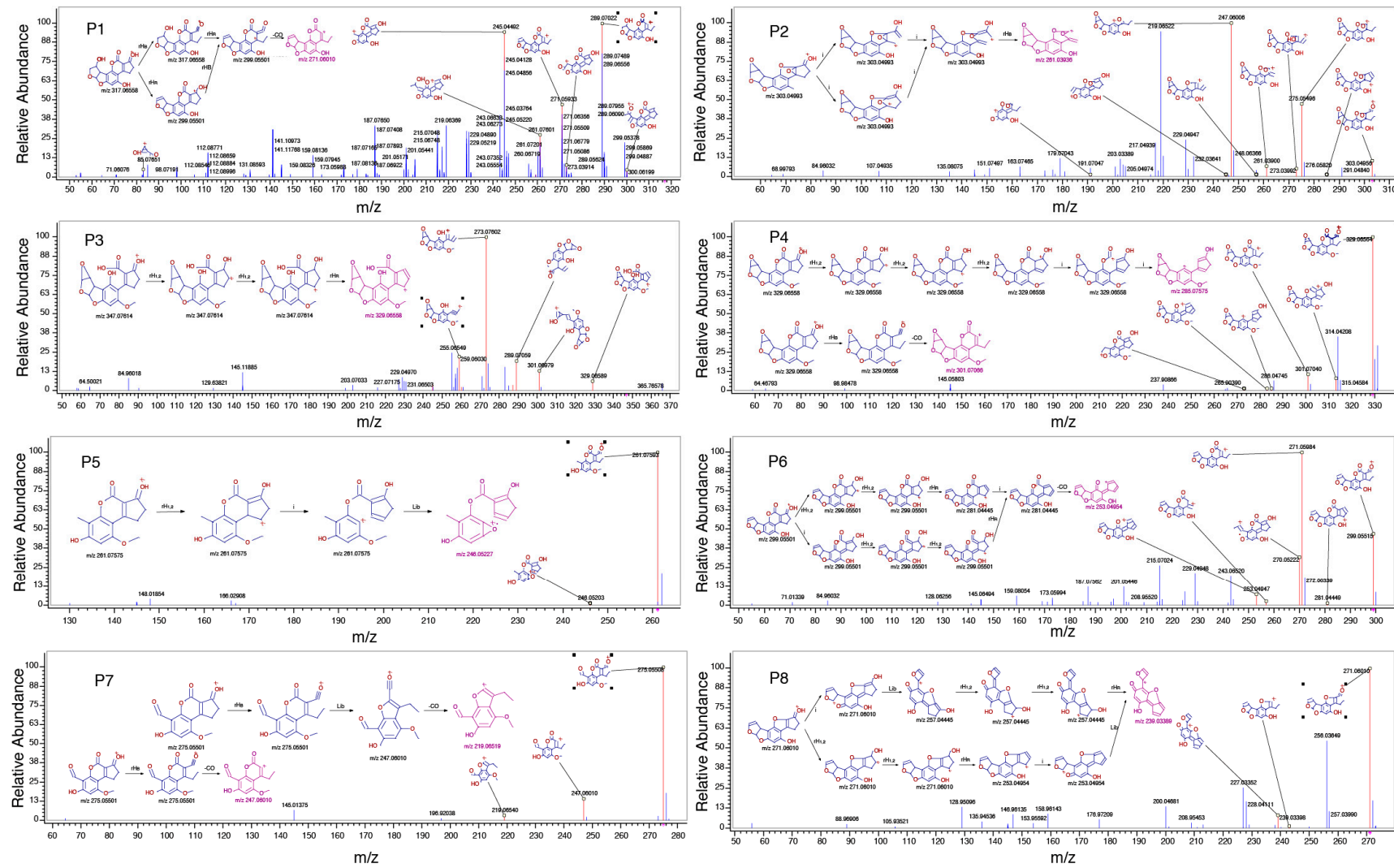
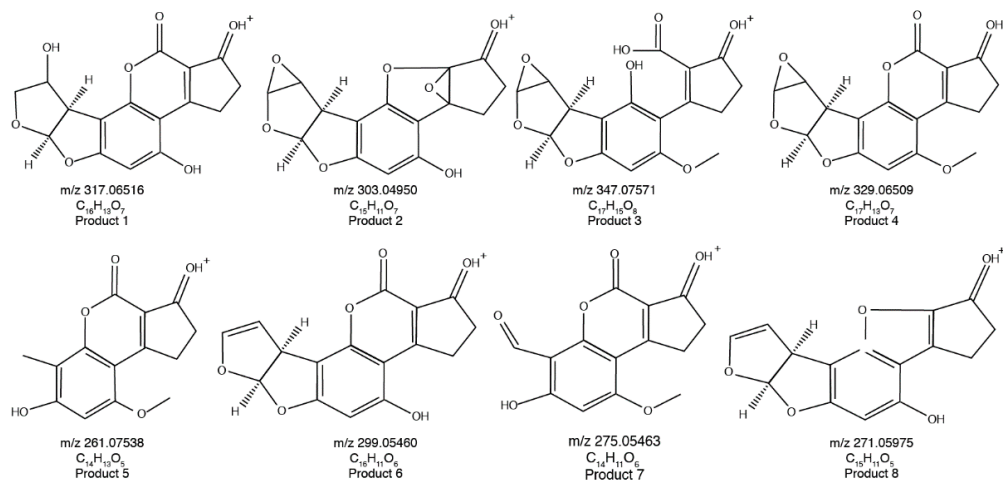
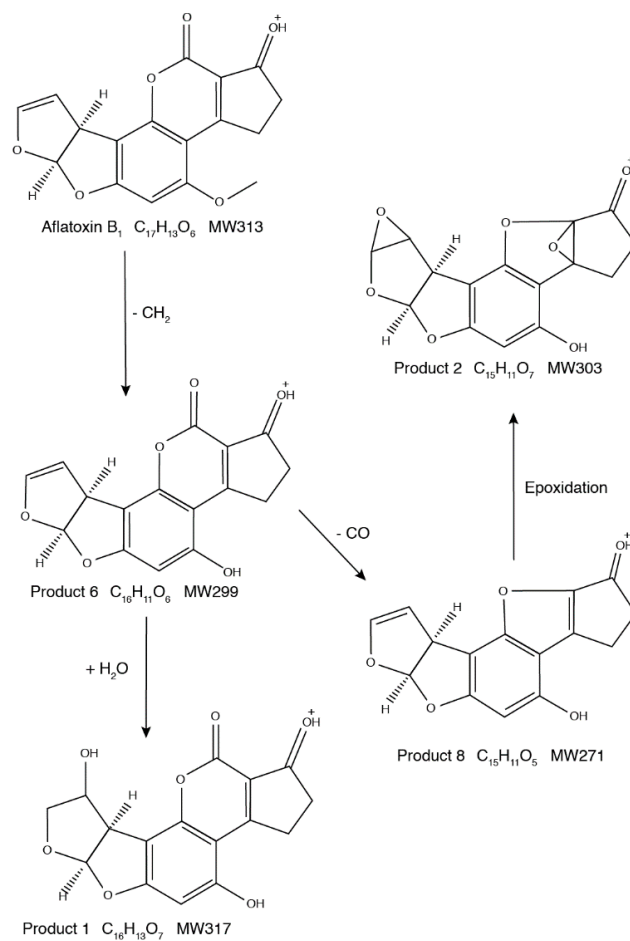


Figure 3. Orbitrap MS-MS spectra and possible fragmentation (insets) of the reaction products of AFB<sub>1</sub> upon ultrasound treatment.



**Figure 4.** Proposed structures of the reaction products (P1–P8) of AFB<sub>1</sub> generated upon ultrasound treatment.

Based on the structures of the eight AFB<sub>1</sub> reaction products generated upon ultrasound treatment, two degradation pathways were proposed (Figures 5 and 6). In the first, AFB<sub>1</sub> is degraded to C<sub>16</sub>H<sub>13</sub>O<sub>7</sub> (*m/z* 317.06516), C<sub>15</sub>H<sub>11</sub>O<sub>7</sub> (*m/z* 303.04950), C<sub>16</sub>H<sub>11</sub>O<sub>6</sub> (*m/z* 299.05460), and C<sub>15</sub>H<sub>11</sub>O<sub>5</sub> (*m/z* 271.05975). In the second, AFB<sub>1</sub> is degraded to C<sub>17</sub>H<sub>15</sub>O<sub>8</sub> (*m/z* 347.07571), C<sub>17</sub>H<sub>13</sub>O<sub>7</sub> (*m/z* 329.06509), C<sub>14</sub>H<sub>13</sub>O<sub>5</sub> (*m/z* 261.07538), and C<sub>14</sub>H<sub>11</sub>O<sub>6</sub> (*m/z* 275.05463).



**Figure 5.** First degradation pathway of AFB<sub>1</sub> under ultrasound treatment.

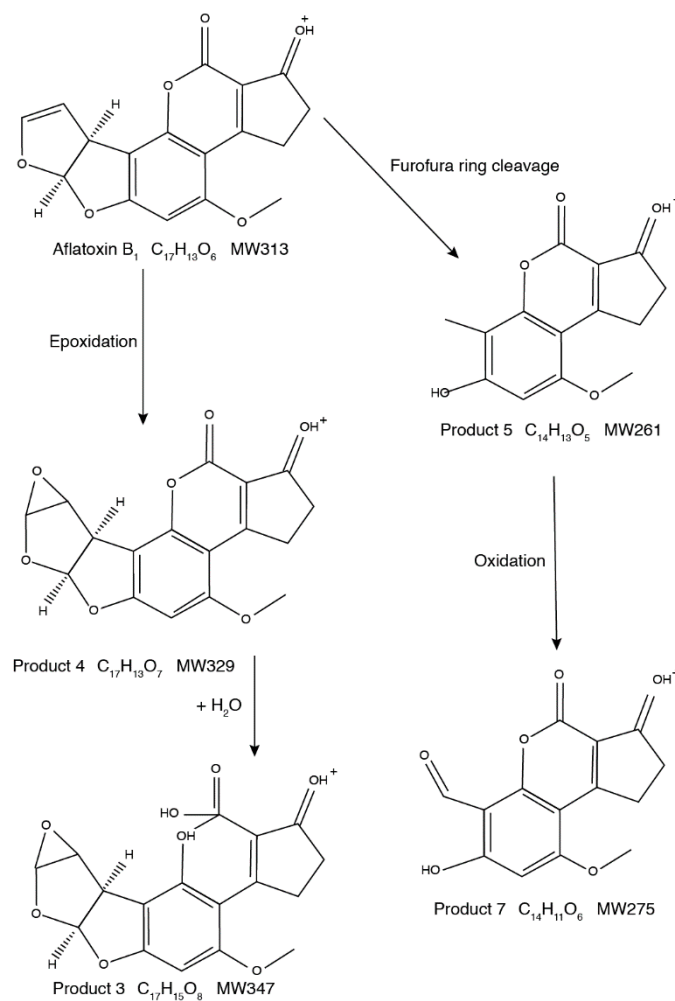


**Figure 6.** Second degradation pathway of AFB<sub>1</sub> under ultrasound treatment.

The first pathway involves mainly the loss of methyl and methanol groups, additions, and epoxidations. The first step is the loss of the methyl residue on the methoxy group on the benzene side chain to form C<sub>16</sub>H<sub>11</sub>O<sub>6</sub> ( $m/z$  299.05460). The next reaction has two branches. In the first, the C8=C9 double bond of AFB<sub>1</sub> is hydrated to produce C<sub>16</sub>H<sub>13</sub>O<sub>7</sub> ( $m/z$  317.06516). In the second, methanol is lost from the lactone ring to generate C<sub>15</sub>H<sub>11</sub>O<sub>5</sub> ( $m/z$  271.05975). Epoxidation of the double bonds in C<sub>15</sub>H<sub>11</sub>O<sub>5</sub> leads to the formation of C<sub>15</sub>H<sub>11</sub>O<sub>7</sub> ( $m/z$  303.04950). Based on the first pathway of AFB<sub>1</sub> degradation, the essential factors are the hydrogen atom (H•), hydroxyl radical (OH•), and hydrogen peroxide. These molecules originated from water molecules that were broken down by the ultrasound treatment [24]. The hydrogen atom and the hydroxyl radical form new reaction products by hydration and hydrogenation. Hydrogen peroxide, which is also generated by ultrasound treatment, contributes to epoxidations.

The second pathway involves mainly epoxidations, oxidations, and additions. The left branch leads to the formation of C<sub>17</sub>H<sub>13</sub>O<sub>7</sub> ( $m/z$  329.06509) through epoxidation of the C8=C9 double bond of AFB<sub>1</sub>. Epoxidation is driven by the hydrogen peroxide generated during ultrasound treatment. Hydrogen peroxide reacts with double bonds and leads to the formation of epoxides [29,30]. Adding water molecules to the double bond at the lactone ring (hydration) produces C<sub>17</sub>H<sub>15</sub>O<sub>8</sub> ( $m/z$  347.07571). In the other branch, the furofuran ring in the AFB<sub>1</sub> molecule is broken down and C<sub>14</sub>H<sub>13</sub>O<sub>5</sub> ( $m/z$  261.07538) is generated. Further oxidation of this by-product contributes to the formation of C<sub>14</sub>H<sub>11</sub>O<sub>6</sub> ( $m/z$  275.05463).

Ultrasonic waves can break down oxygen gas molecules dissolved in water [31]. Several studies have shown that ultrasound bombardment of water generates hydroxyl (OH•), hydrogen atoms (H•), and hydrogen peroxide [32,33]. As the concentrations of these species were not quantified during ultrasound treatment, it is unknown which species reacted with AFB<sub>1</sub>. Probably, the degradation of AFB<sub>1</sub> occurs through uniting all these species, because they coexist during the ultrasound process and are interconvertible. In summary, the second degradation pathway involves epoxidation by H<sub>2</sub>O<sub>2</sub> and oxidation through the combined effects of H•, OH•, and H<sub>2</sub>O<sub>2</sub>.

### 2.5. Toxicity of the Reaction Products

The toxicity of aflatoxins has been extensively investigated since their discovery in the early 1960s [34–36]. Structure-bioactivity relationships of aflatoxins have also been analyzed [37,38]. The molecular structure of AFB<sub>1</sub> is conducive to causing severe toxicity, mutagenicity, and carcinogenicity. Changes in the furofuran or lactone rings or the cyclopentenone or methoxy moieties would markedly reduce the biological activity of AFB<sub>1</sub> [38]. In the present study, IHD was calculated based on the data obtained by Q-Orbitrap and indicated the number of double bonds and rings in the molecule. The IHD of AFB<sub>1</sub> is 11.5. Table 1 shows that the IHDs of 75% of the AFB<sub>1</sub> reaction products were lower than 11.5. As certain reaction products had IHD = 9.5 and others had IHD = 10.5, double bond additions were thought to have occurred. There are two sites on the AFB<sub>1</sub> molecule essential for its toxicity: One is located at the C8=C9 double bond of the furan ring wherein aflatoxin-DNA, and aflatoxin-protein interactions occur; the other is situated at the lactone ring. It is shown in Figure 4 that six of the eight proposed major AFB<sub>1</sub> reaction products showed changes in their double bonds and were very different from AFB<sub>1</sub> via further modifications of the furofuran ring (P-1–P-5 and P-7), lactone ring (P-2, P-3, and P-8), and methoxy group (P-1, P-2, P-6, and P-8). Based on the structure-bioactivity relationships, we believe that the toxicity of the products of ultrasound-treated AFB<sub>1</sub> will be markedly lower than that of AFB<sub>1</sub> itself.

The aforementioned findings were confirmed by an earlier study on AFB<sub>1</sub> treated with aqueous ozone. In those papers, the toxicity of the AFB<sub>1</sub> reaction products was substantially lower or even negligible relative to that of AFB<sub>1</sub> itself [39,40]. Nevertheless, we recommend that additional bioactivity tests, such as duckling and Ames, or cell model studies be conducted to verify that ultrasound-treated AFB<sub>1</sub> samples are safe for animals and humans.

The reaction products generated from pure AFB<sub>1</sub> exposed to ultrasound are complex. In the present study, ultra-high-performance liquid chromatography Q-Orbitrap mass spectrometry (UHPLC-Orbitrap-MS) proved to be the most suitable tool for the elucidation of these breakdown products of AFB<sub>1</sub>. Accurate mass measurements by Orbitrap-MS clarified the elemental composition of the ions (molecules and fragments), while SIEVE v. 2.0 and Mass Frontier v. 7.0 furnished complementary structural information. In the present study, the structures of eight key reaction products of AFB<sub>1</sub> and two possible reaction pathways were proposed. The structures of these by-products suggest that free radical participate in AFB<sub>1</sub> degradation. A toxicity assessment of these reaction products has also been offered. As additional reactions occurred in the formation of most of the reaction products, the toxicity of these compounds were considerably lower than that of AFB<sub>1</sub>.

The findings of the present study present pulsed ultrasound treatment as a promising method to degrade AFB<sub>1</sub> under specific conditions, including in aqueous solutions. In the future, we would like to extend our research to gain insights into how the ultrasound technology works in a food matrix, such as corn or peanuts.

## 3. Materials and Methods

### 3.1. Chemicals and Reagents

Aflatoxin B<sub>1</sub> (purity > 98%) was purchased from J&K Chemical Ltd. (Shanghai, China). Aflatoxin B<sub>1</sub> stock standard solution (100 mg·L<sup>-1</sup>) was prepared by weighing out exactly 5 mg AFB<sub>1</sub> powder

and dissolving it in 50 mL MS-grade acetonitrile. The AFB<sub>1</sub> stock standard solution was stored in a freezer at  $-18\text{ }^{\circ}\text{C}$  before experimental use. Aflatoxin B<sub>1</sub> sample solution ( $10\text{ mg}\cdot\text{L}^{-1}$ ) was prepared by evaporating 2.5-mL aliquots of the standard stock solution and re-dissolving them in 25 mL ultrapure water. LC-MS-grade methanol and acetonitrile were purchased from Thermo Fisher Scientific. Formic acid (purity > 98%) was obtained from Panera (Barcelona, Spain). Water (resistivity =  $18.2\text{ M}\Omega\cdot\text{cm}$ ,  $25\text{ }^{\circ}\text{C}$ ) was produced by an ultrapure purification system (EMD Millipore, Billerica, MA, USA).

### 3.2. AFB<sub>1</sub> Treatment with Power Ultrasound

Each 25-mL Aflatoxin B<sub>1</sub> sample solution was placed in a 50-mL beaker. The probe of the ultrasonic processor was immersed into the sample solutions to a depth of 1.5 cm, and vibration was initiated for the ultrasound experiments. A 550-W power ultrasonic instrument (Branson Ultrasonic Co., Shanghai, China) with a 13-mm probe was used for the ultrasound treatment. The frequency was a constant 20 kHz. The energy input was calculated as the average power per unit volume of the water samples ( $\text{W}\cdot\text{cm}^{-3}$ ). Several preliminary trials were run to determine the most suitable power intensity; for AFB<sub>1</sub> degradation, this was determined to be  $6.6\text{ W}\cdot\text{cm}^{-3}$ . The treatment was carried out in pulsed mode. The AFB<sub>1</sub> samples were treated for 30, 40, 60, or 80 min at a power intensity of  $6.6\text{ W}\cdot\text{cm}^{-3}$  and the treatments were conducted in triplicate. The processed sample solutions were transferred to 25-mL volumetric flasks. To compensate for evaporation during the ultrasonic treatment, ultrapure water was added to certain volumetric flasks to restore the sample solutions to their original 25 mL.

### 3.3. UHPLC–MS Analysis

Ultrasound-treated and untreated AFB<sub>1</sub> samples in ultrapure water were carefully evaporated, re-dissolved in methanol:water (25:75), vortexed for 1 min, and centrifuged at  $4\text{ }^{\circ}\text{C}$  for 10 min at  $12,000\times g$ . One milliliter of the supernatant was then placed into the UHPLC-MS/MS system. The UHPLC-MS/MS system was supplied by Thermo Fisher Scientific. The chromatographic instrument was fitted with an Acquity C18 column ( $100\text{ mm}\times 2.1\text{ mm}$ ) with  $1.7\text{-}\mu\text{m}$  particle size. The Q-Orbitrap mass spectrometer was an MS/MS detector.

Chromatographic analyses were performed by gradient elution. Eluent A was acetonitrile with 0.1% formic acid, and eluent B was an aqueous solution of 0.1% formic acid. Gradient elution began with 10% A for 1 min, which was linearly increased up to 95% in 20.0 min. Then, this status was held for another 1.0 min, returned to 10% eluent A in 1.0 min, and re-equilibrated for another 7.0 min. The flow rate was  $0.30\text{ mL}\cdot\text{min}^{-1}$ , and the column temperature was maintained at  $35\text{ }^{\circ}\text{C}$ . Ten microliters aliquots of the sample extract were placed into the chromatographic system. The MS was operated in positive electrospray ionization (ESI) mode, and the data were obtained within 50–1100  $m/z$ .

### 3.4. UHPLC-MS/MS Analysis

The operational parameters of mass spectrometry were a spray voltage of 3.0 kV, heater temperature of  $350\text{ }^{\circ}\text{C}$ , and a capillary temperature of  $250\text{ }^{\circ}\text{C}$ . The flow rates of the sheath and auxiliary gases were 25 and 5 arb. units, respectively. Dissociation was induced using Ar as the collision gas in the collision cell. High mass accuracy fragmentation data were collected in the data-dependent scanning mode. Data were gained in a full-scan analysis with a resolution of 70,000. The original spectral data were collected and analyzed with Xcalibur v. 3.0, the reaction products were screened with SIEVE v. 2.0, and Mass Frontier v. 7.0 was used to predict the degradation path (all from Thermo Fisher Scientific).

### 3.5. Statistical Analyses

All data were compared using analysis of variance (ANOVA). When the data were considered statistically significant, differences between means were determined using Duncan's multiple range post hoc tests ( $p < 0.05$ ). The statistical analyses were calculated using Statistical Product and Service Solutions (SPSS, 2010) software (IBM, Arundel City, NY, USA).

**Author Contributions:** Conceptualization, Y.L. (Yuanfang Liu) and K.B.; Methodology, Y.L. (Yuanfang Liu), M.L., and Y.L. (Yuanxiao Liu) Software, K.B. and M.L.; Validation, Y.L. (Yuanfang Liu) and Y.L. (Yuanxiao Liu); Formal Analysis, Y.L. (Yuanfang Liu) and M.L.; Investigation, Y.L. (Yuanfang Liu); Resources, K.B.; Data Curation, Y.L. (Yuanfang Liu); Writing—Original Draft Preparation, Y.L. (Yuanfang Liu); Writing—Review and Editing, Y.L. (Yuanfang Liu), K.B., M.L., and Y.L. (Yuanxiao Liu); Visualization, Y.L. (Yuanfang Liu); Supervision, M.L. and K.B.; Project administration, K.B.; Funding acquisition, M.L. and K.B.

**Funding:** This work was supported by the National Modern Agricultural Industry Technology System Construction Program [grant number: CARS-03]; National Natural Science Foundation of China (NSFC) [grant numbers: 31801654]; Startup Funding for PhD of Henan University of Technology [grant numbers: 2017BS018]; and Scientific Research Fund of Henan University of Technology [grant numbers: 2017QNJH15].

**Acknowledgments:** The authors would like to thank Editage [[www.editage.cn](http://www.editage.cn)] for English language editing.

**Conflicts of Interest:** The authors declare no conflict of interest. The sponsors had no role in the design, execution, interpretation, or writing of the study.

## References

1. Battilani, P. Food mycology—a multifaceted approach to fungi and food. *World Mycotoxin J.* **2008**, *1*, 223–224. [[CrossRef](#)]
2. Magan, N.; Olsen, M. Rapid detection of mycotoxigenic fungi in plants. In *Mycotoxins in Food*; Magan, N., Olsen, M., Eds.; Woodhead Publishing: Cambridge, UK, 2004; pp. 111–136.
3. Pitt, J.I. Food mycology: A discipline comes of age. *Food Aust.* **1996**, *48*, 258–261.
4. Kujawa, M. Some naturally occurring substances: Food items and constituents, heterocyclic aromatic amines and mycotoxins. *Mol. Nutr. Food Res.* **1994**, *38*, 351. [[CrossRef](#)]
5. Williams, J.H.; Phillips, T.D.; Jolly, P.E.; Stiles, J.K.; Jolly, C.M.; Aggarwal, D. Human aflatoxicosis in developing countries: A review of toxicology, exposure, potential health consequences, and interventions. *Am. J. Clin. Nutr.* **2004**, *80*, 1106–1122. [[CrossRef](#)] [[PubMed](#)]
6. Fandohan, P.; Gnonlonfin, B.; Hell, K.; Marasas, W.F.; Wingfield, M.J. Natural occurrence of *Fusarium* and subsequent fumonisin contamination in preharvest and stored maize in Benin, West Africa. *Int. J. Food Microbiol.* **2005**, *99*, 173–183. [[CrossRef](#)]
7. Karlovsky, P. Biological detoxification of fungal toxins and its use in plant breeding, feed and food production. *Nat. Toxins* **1999**, *7*, 1–23. [[CrossRef](#)]
8. Karlovsky, P.; Suman, M.; Berthiller, F.; De Meester, J.; Eisenbrand, G.; Perrin, I.; Oswald, I.P.; Speijers, G.; Chiodini, A.; Recker, T.; et al. Impact of food processing and detoxification treatments on mycotoxin contamination. *Mycotoxin Res.* **2016**, *32*, 179–205. [[CrossRef](#)]
9. Liu, R.; Wang, R.; Jian, L.; Chang, M.; Jin, Q.; Du, Z.; Wang, S.; Li, Q.; Wang, X. Degradation of AFB1 in aqueous medium by electron beam irradiation: Kinetics, pathway and toxicology. *Food Control* **2016**, *66*, 151–157. [[CrossRef](#)]
10. Méndez-Albores, A.; Moreno-Martínez, E.; Martínez-Bustos, F.; Gaytán-Martínez, M. Effect of lactic and citric acid on the stability of B-aflatoxins in extrusion-cooked sorghum. *Lett. Appl. Microbiol.* **2008**, *47*, 1–7. [[CrossRef](#)]
11. Inan, F.; Pala, M.; Doymaz, I. Use of ozone in detoxification of aflatoxin B in red pepper. *J. Stored Prod. Res.* **2007**, *43*, 425–429. [[CrossRef](#)]
12. Sakudo, A.; Toyokawa, Y.; Misawa, T.; Imanishi, Y. Degradation and detoxification of aflatoxin B1 using nitrogen gas plasma generated by a static induction thyristor as a pulsed power supply. *Food Control* **2017**, *73*, 619–626. [[CrossRef](#)]
13. Escobedo-González, R.; Méndez-Albores, A.; Villarreal-Barajas, T.; Aceves-Hernández, J.M.; Miranda-Ruvalcaba, R.; Nicolás-Vásquez, I. A theoretical study of 8-chloro hydroxy-aflatoxin B1, the conversion product of aflatoxin B1 by neutral electrolyzed water. *Toxins* **2016**, *8*, 225. [[CrossRef](#)] [[PubMed](#)]
14. Somayajula, A.; Asaithambi, P.; Susree, M.; Matheswaran, M. Sono-electrochemical oxidation for decolorization of Reactive Red 195. *Ultrason. Sonochem.* **2012**, *19*, 803–811. [[CrossRef](#)] [[PubMed](#)]
15. De Lima Leite, R.H.; Cognet, P.; Wilhelm, A.-M.; Delmas, H. Anodic oxidation of 2,4-dihydroxybenzoic acid for wastewater treatment: Study of ultrasound activation. *Chem. Eng. Sci.* **2002**, *57*, 767–778. [[CrossRef](#)]
16. Suslick, K.S.; Nyborg, W.L. Ultrasound: Its chemical, physical and biological effects. *J. Acoust. Soc. Am.* **1990**, *87*, 919–920. [[CrossRef](#)]

17. Yao, J.J.; Gao, N.Y.; Deng, Y.; Ma, Y.; Li, H.-J.; Xu, B.; Li, L. Sonolytic degradation of parathion and the formation of byproducts. *Ultrason. Sonochem.* **2010**, *17*, 802–809. [[CrossRef](#)] [[PubMed](#)]
18. Kim, D.K.; He, Y.; Jeon, J.; O'Shea, K.E. Irradiation of ultrasound to 5 methylbenzotriazole in aqueous phase: Degradation kinetics and mechanisms. *Ultrason. Sonochem.* **2016**, *31*, 227–236. [[CrossRef](#)] [[PubMed](#)]
19. Musmarra, D.; Prisciandaro, M.; Capocelli, M.; Karatza, D.; Lovino, P.; Canzano, S.; Lancia, A. Degradation of ibuprofen by hydrodynamic cavitation: Reaction pathways and effect of operational parameters. *Ultrason. Sonochem.* **2016**, *29*, 76–83. [[CrossRef](#)] [[PubMed](#)]
20. Papadopoulos, C.; Frontistis, Z.; Antonopoulou, M.; Venieri, D.; Konstantinou, I.; Mantzavinos, D. Sonochemical degradation of ethyl paraben in environmental samples: Statistically important parameters determining kinetics, by-products and pathways. *Ultrason. Sonochem.* **2016**, *31*, 62–70. [[CrossRef](#)]
21. Liu, Y.; Li, M.; Liu, Y.; Bai, F.; Bian, K. Effects of pulsed ultrasound at 20 kHz on the sonochemical degradation of mycotoxins. *World Mycotoxin J.* **2019**. [[CrossRef](#)]
22. Mason, T.J.; Chemat, F.; Vinatoru, M. The extraction of natural products using ultrasound or microwaves. *Curr. Org. Chem.* **2011**, *15*, 237–247. [[CrossRef](#)]
23. Zheng, H.; Wei, S.; Xu, Y.; Fan, M. Reduction of aflatoxin B1 in peanut meal by extrusion cooking. *LWT Food Sci. Technol.* **2015**, *64*, 515–519. [[CrossRef](#)]
24. Ince, N.H. Ultrasound-assisted advanced oxidation processes for water decontamination. *Ultrason. Sonochem.* **2018**, *40*, 97–103. [[CrossRef](#)] [[PubMed](#)]
25. Thompson, L.H.; Doraiswamy, L.K. Sonochemistry: Science and engineering. *Ind. Eng. Chem. Res.* **1999**, *38*, 1215–1249. [[CrossRef](#)]
26. Luo, X.; Wang, R.; Wang, L.; Wang, Y.; Chen, Z. Structure elucidation and toxicity analyses of the degradation products of aflatoxin B-1 by aqueous ozone. *Food Control* **2013**, *31*, 331–336. [[CrossRef](#)]
27. Zorlugenç, B.; Zorlugenç, F.K.; Öztekin, S.; Evliya, I.B. The influence of gaseous ozone and ozonated water on microbial flora and degradation of aflatoxin B1 in dried figs. *Food Chem. Toxicol.* **2008**, *46*, 3593–3597. [[CrossRef](#)] [[PubMed](#)]
28. Enjie, D.; Changpo, S.; Hanxue, H.; Shanshan, W.; Minghua, L.; Haizhou, D. Structures of the ozonolysis products and ozonolysis pathway of aflatoxin B1 in acetonitrile solution. *J. Agric. Food Chem.* **2012**, *60*, 9364–9370. [[CrossRef](#)]
29. Shi, H.; Cooper, B.R.; Stroshine, R.L.; Iteleji, K.E.; Keener, K. Structures of degradation products and degradation pathways of aflatoxin b1 by high voltage atmospheric cold plasma (HVACP) treatment. *J. Agric. Food Chem.* **2017**, *65*, 6222–6230. [[CrossRef](#)]
30. Koelewijn, P. Epoxidation of olefins by alkylperoxy radicals. *Recl. Trav. Chim. Pays Bas* **2010**, *91*, 759–779. [[CrossRef](#)]
31. Hart, E.J.; Henglein, A. Sonolysis of ozone in aqueous solution. *J. Phys. Chem.* **1986**, *90*, 3061–3062. [[CrossRef](#)]
32. Authier, O.; Ouhabaz, H.; Bedogni, S. Modeling of sonochemistry in water in the presence of dissolved carbon dioxide. *Ultrason. Sonochem.* **2018**, *45*, 17–18. [[CrossRef](#)] [[PubMed](#)]
33. Reuter, F.; Lesnik, S.; Ayaz-Bustami, K.; Brenner, G.; Mettin, R. Bubble size measurements in different acoustic cavitation structures: Filaments, clusters, and the acoustically cavitated jet. *Ultrason. Sonochem.* **2019**, *55*, 383–394. [[CrossRef](#)] [[PubMed](#)]
34. Baertschi, S.W.; Raney, K.D.; Stone, M.P.; Harris, T.M. ChemInform abstract: Preparation of the 8,9-epoxide of the mycotoxin aflatoxin B1: The ultimate carcinogenic species. *ChemInform* **1989**, *20*. [[CrossRef](#)]
35. Johnson, W.W.; Guengerich, F.P. Reaction of aflatoxin B1 exo-8,9-epoxide with DNA: Kinetic analysis of covalent binding and DNA-induced hydrolysis. *Proc. Natl. Acad. Sci. USA* **1997**, *94*, 6121–6125. [[CrossRef](#)] [[PubMed](#)]
36. Kensler, T.W.; Roebuck, B.D.; Wogan, G.N.; Groopman, J.D. Aflatoxin: A 50 year odyssey of mechanistic and translational toxicology. *Toxicol. Sci.* **2011**, *120*, S28–S48. [[CrossRef](#)] [[PubMed](#)]
37. Lee, L.S.; Dunn, J.J.; Delucca, A.J.; Ciegler, A. Role of lactone ring of aflatoxin B1 in toxicity and mutagenicity. *Experientia* **1981**, *37*, 16–17. [[CrossRef](#)] [[PubMed](#)]
38. Wogan, G.N.; Edwards, G.S.; Newberne, P.M. Structure-activity relationships in toxicity and carcinogenicity of aflatoxins and analogs. *Cancer Res.* **1971**, *31*, 1936–1942. [[PubMed](#)]

39. Feng, W.; Fang, X.; Xiaofeng, X.; Wang, Z.; Fan, B.; Ha, Y. Structure elucidation and toxicity analyses of the radiolytic products of aflatoxin B1 in methanol-water solution. *J. Hazard Mater.* **2011**, *192*, 1192–1202. [[CrossRef](#)]
40. Mao, J.; He, B.; Zhang, L.; Li, P.; Zhang, Q.; Ding, X.; Zhang, W. A structure identification and toxicity assessment of the degradation products of aflatoxin B<sub>1</sub> in peanut oil under UV irradiation. *Toxins* **2016**, *8*, 332. [[CrossRef](#)]



© 2019 by the authors. Licensee MDPI, Basel, Switzerland. This article is an open access article distributed under the terms and conditions of the Creative Commons Attribution (CC BY) license (<http://creativecommons.org/licenses/by/4.0/>).